

## Article

# Investigations on the Potential of 5G for the Detection of Wear in Industrial Roller-Burnishing Processes

Maximilian Kosel <sup>1,\*</sup>, Tobias Schippers <sup>2</sup>, Aziz Abdul <sup>1</sup>, Kristina Ishii <sup>1</sup>, Jacek Mainczyk <sup>2</sup>, Jürgen Mansel <sup>2</sup>, Kai Milnikel <sup>2</sup>, Bünyamin Nurkan <sup>3</sup>, Ralf Löschner <sup>3</sup>, Konstantin Haefner <sup>3</sup>, Daniel Zontar <sup>1</sup> and Christian Brecher <sup>1,4</sup>

- <sup>1</sup> Fraunhofer Institute for Production Technology IPT, 52074 Aachen, Germany; abdul.aziz.abdul.sahul.hamid@ipt.fraunhofer.de (A.A.); kristina.ishii@ipt.fraunhofer.de (K.I.); daniel.zontar@ipt.fraunhofer.de (D.Z.); christian.brecher@ipt.fraunhofer.de (C.B.)
- <sup>2</sup> R&D Steuerungstechnik GmbH & Co. KG, 41189 Mönchengladbach, Germany; tobias.schippers@rud.info (T.S.); jacek.mainczyk@rud.info (J.M.); juergen.mansel@rud.info (J.M.); kai.milnikel@rud.info (K.M.)
- <sup>3</sup> Wenaroll GmbH Tools and Systems, 42799 Leichlingen, Germany; b.nurkan@wenaroll.de (B.N.); r.loeschner@wenaroll.de (R.L.); info@wenaroll.de (K.H.)
- <sup>4</sup> Werkzeugmaschinenlabor (WZL), RWTH Aachen University, 52074 Aachen, Germany
- \* Correspondence: maximilian.kosel@ipt.fraunhofer.de

**Abstract:** Roller burnishing represents an economical alternative to conventional surface-finishing processes, such as fine turning or honing. In contrast to the well-known wear mechanisms of chip-forming processes, the wear behavior in roller-burnishing is strongly based on the experience of the machine operators. The nature of the finishing process makes roller-burnishing very sensitive to surface defects, as it is often not possible to rework the last step in a process chain. In the present work, a prototype for a smart roller-burnishing tool with 5G communication is presented, which serves as an inline-monitoring tool to detect tool wear. A suitable metric to monitor the tool wear of the manufacturing roll is suggested, and the potentials of 5G communication for the described use-case are evaluated. Based on the signal-to-noise ratio of the process-force, a metric is found that distinguishes new rolls from worn rolls with very small defects on the micrometer scale. Using the presented approach, it was possible to distinguish the signal-to-noise ratio of a roll with very small wear marks by 3.8% on average. In the case of stronger wear marks, on the order of 20  $\mu\text{m}$ , the difference increased to up to 15.6%.

**Keywords:** roller-burnishing; burnishing; 5G; surface finishing



**Citation:** Kosel, M.; Schippers, T.; Abdul, A.; Ishii, K.; Mainczyk, J.; Mansel, J.; Milnikel, K.; Nurkan, B.; Löschner, R.; Haefner, K.; et al. Investigations on the Potential of 5G for the Detection of Wear in Industrial Roller-Burnishing Processes. *Electronics* **2022**, *11*, 1678. <https://doi.org/10.3390/electronics11111678>

Academic Editor: Domenico Mazzeo

Received: 29 April 2022

Accepted: 21 May 2022

Published: 25 May 2022

**Publisher's Note:** MDPI stays neutral with regard to jurisdictional claims in published maps and institutional affiliations.



**Copyright:** © 2022 by the authors. Licensee MDPI, Basel, Switzerland. This article is an open access article distributed under the terms and conditions of the Creative Commons Attribution (CC BY) license (<https://creativecommons.org/licenses/by/4.0/>).

## 1. Introduction

Finishing operations are the last step in most manufacturing process chains and are often crucial for the quality of the manufactured part. Demanding industrial specifications originating, e.g., from the automotive industry or the construction machinery sector, require semi-finished workpieces with the highest surface qualities below 1  $\mu\text{m}$  Rz [1]. In order to produce high-throughput products, such as pneumatic or hydraulic cylinders, in the requested tolerances in an economic process, roller-burnishing has become a renowned alternative to other fine-machining processes, such as turning or grinding.

During roller burnishing, the roughness of the machined surface is improved from a pre-machined surface with Rz on the order of tenth of microns down to Rz < 1  $\mu\text{m}$  [2]. In addition, the material contact ratio is significantly increased (over 70%) [3]. This also improves the wear characteristics [4] (p. 65), and the risk of cracking due to micro-notches is also reduced by roller burnishing [5]. Another positive effect of burnishing is the increase of the hardness of the surface layer due to strain-hardening [6]. In contrast to other comparable processes, which are lengthy and environmentally harmful, such as honing, roller burnishing is cost-effective, fast and sustainable.

The burnishing process does not cause any material removal, the lubricant requirement is minimized, and noise emissions are reduced. The roller burnishing process is economical compared to grinding, honing or polishing. A reduction in production costs of more than 50% can be realized, as expensive reworking and expensive purchases, such as machines, can be significantly reduced [7].

During a roller burnishing operation, a small burnishing roll is pressed against a pre-machined, typically cylindrical, workpiece, which is turned around its longitudinal axis [8] (p. 14). Due to the high pressure from the burnishing roll to the workpiece surface, the surface roughness of the workpiece is deformed into a flat surface with a high-quality finish. Figure 1 shows a schematic drawing of a roller-burnishing operation.

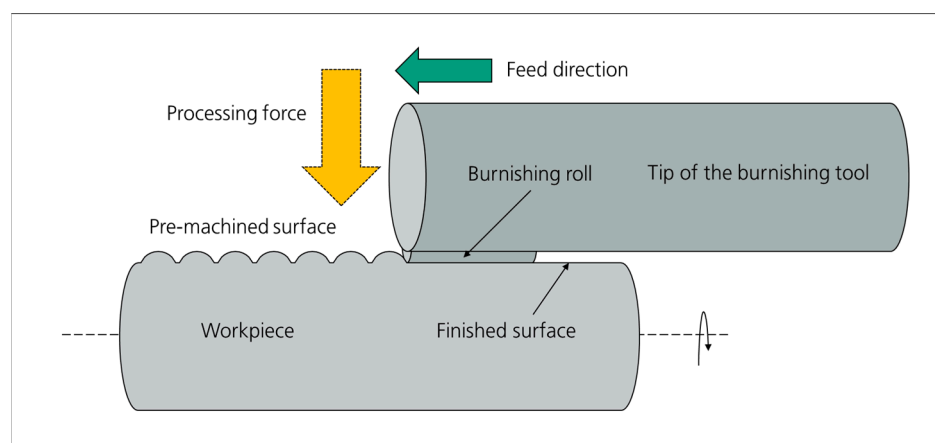


**Figure 1.** Schematic drawing of a roller burnishing process. The burnishing roll is moved over a turning workpiece with a pre-machined surface roughness. Due to high process forces, the roughness of the workpiece is deformed into a flat surface during the burnishing operation. Source: own-elaboration.

While turning, grinding or honing all belong to the class of chip-forming technologies, roller burnishing is a reshaping technology, which offers significantly different wear mechanisms compared to the conventional manufacturing methods. While chip-forming technologies mostly suffer from a reduction of the processing quality due to tool wear and rounding of the cutting edge [9], roller burnishing is vulnerable to wear mechanisms, such as surface distress or pitting, which are usually associated with the research field of bearing analysis. All these finishing operations necessitate the monitoring of tool wear; compare with, e.g., the case of turning [10].

Due to the complex nature of the mentioned wear mechanisms of roller burnishing, there is a strong need for appropriate monitoring technologies of the rollers used during the processing. As high-frequency monitoring is required, and harsh environments in the machines make the use of cables often impractical or even impossible, an appropriate communication system to transmit the data from the point of acquisition (tool) to the motion control of the machine is required. For this purpose, 5G offers significant potential, due to its high reliability and low-latency communication.

In this paper, a tool-wear monitoring approach based on the signal-to-noise ratio of the processing force is presented, which monitors the tool condition based on a wireless communication approach. The benefits of 5G in this application are investigated and benchmarked against standard WiFi for the requirements of the elaborated monitoring mechanism.

After introducing the general concept and motivation (2) behind the project, the paper will give an overview over the materials and methods used (3), then proceed to presenting the results of the experiments (4) and finish with a discussion of the results and an outlook to the future (5).

## 2. General Concept and Motivation

This work is part of the 5G.NRW project RISEN\_5G, which targets the development of a smart roller-burnishing tool, equipped with 5G communication and capable of detecting tool-wear during processing. The impact of the processing force is well elaborated in chip-forming manufacturing processes, such as turning or milling and is usually acquired by dynamometric sensors [11,12].

It is known from preliminary studies that the processing force also has a high impact on the achievable surface quality during the roller burnishing process [13]. As the application of dynamometers is often impractical and demanding regarding the requirements for the data processing, many standard tools are equipped with analog dial gauges to estimate the processing force based on the deformation of the tool. The manufacturing infeed is adjusted until a specified value of the dial gauge is reached and the operation is started.

During the actual roller burnishing operation, there is no feedback available on the processing conditions. Therefore, occurring tool wear is only detected by the production of defect parts. The underlying motivation of the RISEN\_5G project is to move the detection of defect parts from a reactive, manual approach towards an inline wear detection, capable of recognizing the occurrence of unusual tool behavior of the process signals.

At the time this paper was written, a first prototype of the smart burnishing tool was developed, and a suitable metric was elaborated, which enabled differentiation between good rolls and worn rolls. A 5G-based communication concept was developed, which is currently being tested by simulated process data. In parallel, data from real processes is acquired in the facilities of project partner R&D Steuerungstechnik GmbH & Co. KG. Due to the lack of an appropriate 5G-network at the trial site, these trials are performed by using a cable-based solution in an experimental setup.

## 3. Materials and Methods

### 3.1. Machine Tool

The process of roller burnishing mostly takes place using either special-purpose machines or standard lathes. This depends on the process and whether the work piece or tool is rotating.

In the case of this project, the decision was made to use a CNC-lathe to create reproducible test scenarios and establish a realistic, industrial environment. A MONFORTS KNC10plus (Figure 2) was used as the machine tool, which is capable of clamping round stock workpieces up to  $\text{Ø}1100$  by 8000 mm and to apply radial forces up to 12 kN. These key-figures make it suitable for burnishing harder materials while offering a high flexibility and residual capabilities for tests in more extreme conditions. In addition, the usage of a lathe has the benefit that pre-machining as well as the burnishing process can be performed on the same machine tool.



**Figure 2.** Test machine tool—MONFORTS KNC10plus with MTC controller. Source: R&D Steuerungstechnik GmbH & Co. KG.

The KNC10plus is equipped with a numeric control system, MTC, designed and produced by one of the project partners, R&D Steuerungstechnik GmbH & Co. KG. This has the advantage of being able to modify and customize low-level software aspects to rapidly integrate hardware during the early stages of development without the need to start from scratch in the case of varying requirements.

Additionally, the controller offers a variety of connectivity options to attach, for example a TTL-probe via cable. By directly replacing the analogue dial gauge of a standard burnishing tool with a digital linear probe opens a simple way to feed the process force to the controller in order to automate the process of both pre-processing as well as roller burnishing. In initial experiments, a HEIDENHAIN-METRO #MT2571 was used for this purpose.

A CNC program with an input mask was developed (see Figure 3), providing basic functionality to fully parameterize the process, such as the positions, feeds and spindle speed as well as the value seen on the dial gauge. This provides a coordinated approach for the movement and application of the correct force in the beginning. It is possible to record the process data locally, which enables the first insights into the process data.



**Figure 3.** Roller burnishing cycle mask (German edition). Source: R&D Steuerungstechnik GmbH & Co.KG.

For testing purposes, using a wired sensor is a simple and suitable solution, however, is not recommended due to physical limitations and harsh industrial conditions. Therefore, a wireless connection improves this method in terms of waterproof encapsulation and flexible retrofitting to existing machines.

### 3.2. G-Infrastructure

5G is the fifth-generation technology standard for mobile networks, whose worldwide deployment began in 2019. Compared to the previous 4G LTE standard, 5G has significantly higher bandwidth and therefore can offer higher data rates, lower latency, higher reliability and increased network capacity and availability [14] (p. 894).

5G can be implemented in the low-band, mid-band or high-band spectrum [15]. The spectrum below 1 GHz is considered low band. Low-band 5G uses a similar frequency range to 4G, providing latency and download speeds only marginally better than 4G, i.e., reaching 250 megabits per second (Mbit/s) [16]. However, low-band cell towers have a wide range and coverage making it easier for the wireless signal to penetrate windows and walls [17] (pp. 119–122).

The mid-band spectrum is in the 1–6 GHz range. Mid-band 5G uses microwaves allowing speeds up to 1 gigabit-per-second (Gbit/s) [16], with each cell tower providing service up to several kilometers in radius. High-band 5G uses frequencies of 24 GHz or higher, near the bottom of the millimeter wave band. It can achieve download speeds up to 20 Gbit/s [17] (p. 143). However, millimeter waves have a more limited range, sometimes less than a mile, requiring smaller cells, and they are susceptible to interference from buildings and trees [17] (pp. 119–122).

Fraunhofer IPT is part of the 5G-Industry Campus Europe [18], a research infrastructure for the validation of 5G in production at RWTH Aachen Campus Melaten, where three production research institutes—apart from the Fraunhofer IPT, the Machine Tool Laboratory (WZL) at RWTH Aachen University and the Research Institute for Rationalization (FIR) e. V. at RWTH Aachen University—cooperate, thereby, offering a wide range of representative 5G use-cases for industrial applications.

These range from 5G-sensor technology for monitoring and controlling highly complex manufacturing processes to mobile robotics and logistics and cross-location production chains. Further details regarding the different use cases can be found in the following papers [19]. The RISEN\_5G project is independent of those use cases and funded by the Ministry of Economics, Innovation, Digitisation and Energy of the State of North Rhine-Westphalia as part of the 5G.NRW Competence Center [20].

On the shop floor of Fraunhofer IPT, covering an area of 3000 m<sup>2</sup>, three different 5G non-public networks (NPN), i.e., networks at enterprise locations in support of industrial IoT services for industry users as specified by the 5G standard, have been deployed. The 5G network supplier is Ericsson. There are two different 5G Standalone (SA) systems, one operating on the mid-band and one on the high-band spectrum.

The third deployment is a 5G non-standalone system (NSA). The 5G RAN uses 100 MHz of bandwidth in the locally-licensed mid-band Time-Division Duplex (TDD) spectrum at the 3.7–3.8 GHz frequency band (5G band n78) [21] (p. 416). The system uses commercial 5G network components and can thus be used with commercially available terminal devices. The 4G anchor band operates at the 2300 MHz spectrum (4G band B40). Further information about the 5G trial systems can be found in [22].

In this project, the 5G NSA system is used for the communication benchmark. In practice, a non-standalone network will often be the first stage of the step-by-step upgrade of mobile networks to the 5G standard. This is showcased by the infrastructural expansion of 5G-Networks in Germany mostly being performed by an intermediate step over an NSA network towards standalone networks. Thus, NSA networks represent the available option for 5G communication in most companies, due to high financial barriers for company-owned SA networks. Hence, to ensure the most relevant results for industrial purposes, the NSA network was chosen as the benchmark.

### 3.3. Tool Concept

Single-roller burnishing tools are the most flexible type of roller burnishing tools, as they can be used to work on workpieces at the inner- and outer-geometry. Thus, a single-roller tool, manufactured by the project partner Wenaroll GmbH was chosen as the corresponding demonstration tool in this paper.

From preliminary process experience, it is known that the processing force has a significant influence on the manufactured surface quality. For this reason, the front of the tool and the back of the tool are interconnected to each other by flexural sheet-metals, translating the applied processing force to a relative parallel movement between both parts. This translational movement is measured by a high-speed linear scale, and the corresponding signals are transmitted via the network to a gateway at the machine tool. Typical processing forces for roller burnishing processes are on the order of 1–10 kN. Considering the magnitude of the force, a slight bending of the tool cannot be excluded. Therefore, the measuring scale is applied on the side of the tool in a separate mounting point.

Figure 4 depicts the CAD-model of the developed roller burnishing tool.

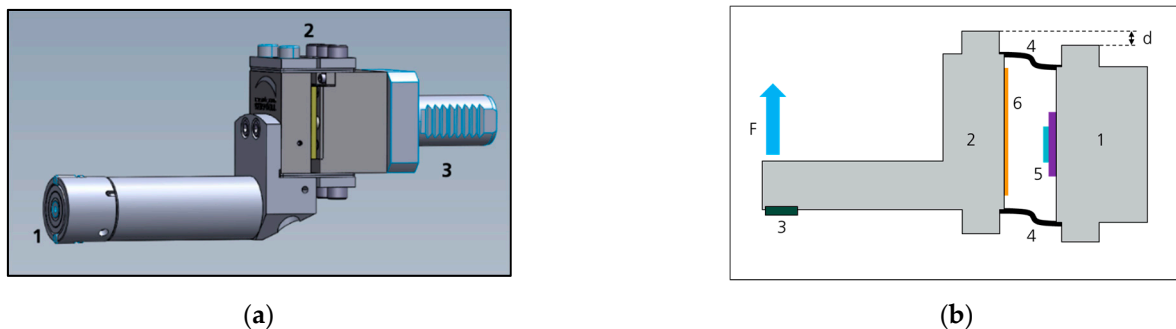


**Figure 4.** CAD models of the developed roller burnishing tool. (a): Side view of the complete tool with active front part (1), middle part with flexural sheet metals (2) and back-part with VDI tool-mounting unit (3). (b): Schematic drawing of the tool with functional parts: 1—Backside of the tool, 2—Frontside of the tool, 3—Roll used for the burnishing operation, 4—Flexural metal sheets, 5—Linear Encoder Head, and 6—Scale. The relative movement between the front and the back part (distance  $d$ ) is measured by the scale to determine the processing force. Source: own-elaboration.

The linear scale is a Renishaw Atom DX sensor with an interpolated resolution of  $0.2 \mu\text{m}$  and a signal acquisition frequency of 40 MHz. The period of the used steel-scale is  $40 \mu\text{m}$ . In order to provide an appropriate signal-acquisition unit for the scale, a STM-32 L452-P low energy microcontroller is used. The microcontroller acquires the scale's signal and transmits it over an existing network to a gateway at the machine tool.

### 3.4. Communication

In order to save bandwidth and provide a stable communication from the tool to the machine-gateway, a custom communication protocol is developed.

#### 3.4.1. Data

Derived from initial trials and user experience, the following data, seen in Table 1, were considered to be the most significant and operation critical. They were sent wirelessly from the tool module to the gateway.

**Table 1.** Datapoints of interest. Types refer to typical C-language variables.

Datapoint	Type/Number of Raw Bytes
encoder-position	float/4
timestamp	short unsigned int/2
status-bits	byte/1
temperature	byte/1
voltage	short int 2

#### 3.4.2. Data Transmission

To ensure a safe and robust transmission, all datapoints are embedded into a single string. Examples can be seen in Tables 2 and 3. Sending each datapoint separately would produce unnecessary overhead or result in uncorrelated pieces of information. The raw values are converted to a hexadecimal format, and thus different ASCII characters (except 0–9 and A–F) can be used as indication characters (start ID). To check whether communication is stable and to have the option to analyze the time-related data (e.g., the first derivative), a checksum and a timestamp are added. To determine the end of a frame, an end ID is appended to the end.

**Table 2.** Full telegram (24 bytes). Depicted are a dummy message and the number of bytes per datapoint.

Start-ID	Time-Stamp	Status Bits	Encoder-Position	Temp.	Battery-Voltage	Check-Sum	End-ID
L	0000	aa	01234567	00	1234	ff	\R
1	4	2	8	2	4	2	1

**Table 3.** Reduced telegram (18 bytes). Depicted are a dummy message and the number of bytes per datapoint.

Start-ID	Timestamp	Status Bits	Encoder-Position	Checksum	End-ID
S	0000	aa	01234567	ff	\R
1	4	2	8	2	1

### 3.4.3. Reduced Real-Time Data Transmission (RT-Data)

Not all data has to be transmitted in real-time. Only the encoder position and status bits are relevant in order to quickly detect and react to any issues. This reduced data frame is sent periodically every 5 ms as depicted in Figure 5. The isochronous type of this transmission simplifies analysis of the data and ensures reliability.

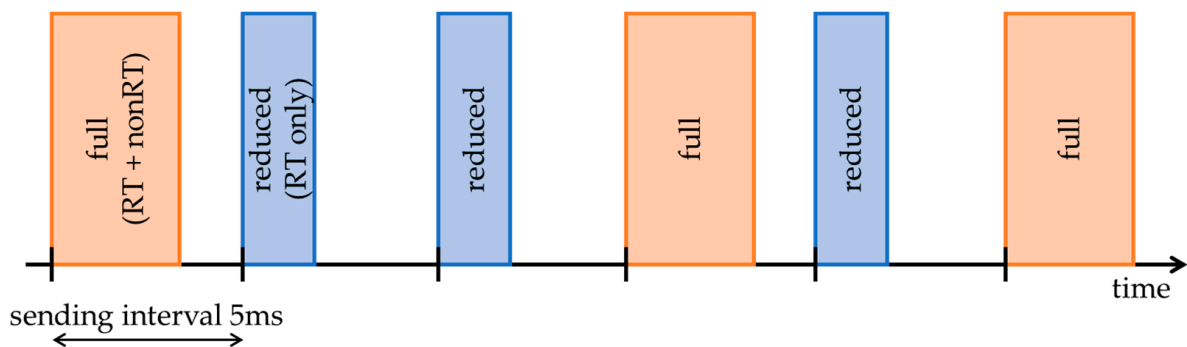


**Figure 5.** Whenever a full package is being sent, it replaces the reduced one. Source: R&D Steuerungstechnik GmbH & Co. KG.

Thus, the reduced transmission excludes temperature and battery voltage, which saves 6 bytes/package (25%). A full package is only sent if a non-RT value has changed or is actively requested, replacing the reduced one. This is different to typical isochronous real-time transmission, where the non-RT data is sent in between two RT packages.

### 3.4.4. Data Exchange between Gateway and -Controller

As the gateway module needs to be able to communicate to the machine, some data has to be sent to the machine controller, the CNC. Thus, the gateway should be able to record and possibly visualize process data, such as the positions of the axes, spindle speed and feed rates. Therefore, a PROFINET-connection is established between them.

Tables 4 and 5 show the individual datapoints and the number of raw bytes when represented as variable in programming language C.

**Table 4.** Data from the gateway module to the controller.

Datapoint	Type/Number of Raw Bytes
process force	float/4
tool module status	byte/1
tool wear in %	byte/1

**Table 5.** Data from the controller to the gateway module.

Datapoint	Type/Number of Raw Bytes
position X-axis in mm	float/4
position Z-axis in mm	float/4
spindle angle in °	float/4
spindle speed in 1/min	float/4
NC program status (acProg) BITS:	
0. program running	
1. prog waiting	
2. prog in Stop	
3. prog interrupted	byte/1
4. burnishing cycle active	
5. burnishing: ongoing process	
6. turn cycle active	
7. NCSTART burnishing	
# Tool ID (name)	string/32

In order to test the 5G-communication, an electronic setup was used that could be deployed as an embedded system in a later stage of the product. The Quctel RMU 500 EK development board, which is based on the RM500Q 5G-chip, was used for the development phase of this product. After compiling the drivers together with a custom Linux kernel, the board was connected to a Raspberry Pi 4B, which represents the client-side of the communication benchmark described in Section 4.2. For the server-side communication, an Ubuntu Linux machine was hosted at the internal hosting service of Fraunhofer, the Fraunhofer Edge Cloud, which is directly connected to the 5G-network infrastructure.

## 4. Results

### 4.1. Experimental Procedure and Data Acquisition

For the conduction of experiments and the evaluation of the acquired signals, the project partner Wenaroll GmbH provided burnishing rolls at different wear levels to measure the differences between the rolls. A cylindrical steel-workpiece (material: 1.4021/X20Cr13) was used as a demonstrator for the experiments. As roller burnishing is a finishing process, the surface of the workpiece was pre-machined before every experiment in a traditional turning process.

After the pre-machining process, a roll was fitted into the burnishing tool, and the corresponding finishing operation was conducted. During all trials, the recommended processing force of 4 kN was used with a feed rate of 0.4 mm/rev (about 360 mm/min for a radius of 30 mm). For the data-acquisition, a high-frequency system made by Fraunhofer IPT, the Fraunhofer vBox, was used. This system provides the possibility to acquire data at high frequencies of up to 100 kHz. With this system, the bending of the tool, as well as the axis positions of the machine tool were acquired with a sampling frequency of 100 kHz. The overall setup and workflow of the experiments is shown in Figure 6.

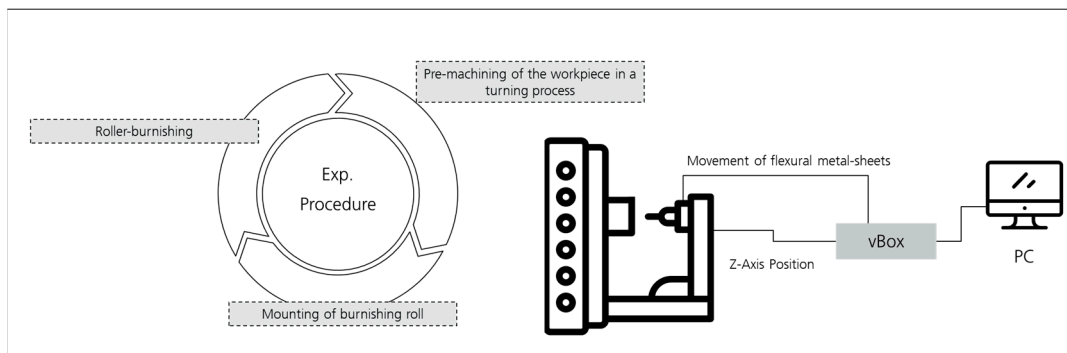


**Figure 6.** Left: Schematic representing the steps of one experiment, consisting of 1, Pre-machining of the workpiece in a turning process; 2, Mounting of the burnishing roll in the burnishing tool; and 3, Finishing operation in roller-burnishing. Right: Schematic of signal acquisition, with the tool deflection and z-axis position acquired from the used machine tool. The data was collected and synchronized by the Fraunhofer vBox and sent to a PC for subsequent processing. Source: own-elaboration.

#### 4.2. Tool-Wear Monitoring by Processing Force

In order to find a quantifiable measure for the wear in the roller burnishing process, worn rolls, collected from industrial companies were classified in an initial benchmark. Essentially, two different kinds of wear mechanisms were observed in which the set of 20 worn rolls was classified. For every category, the visible appearance, as well as a confocal microscope measurement of the wear mechanism is included into the classification.

Category 1 consists of rolls that show visible and measurable groove-marks. Under the microscope, these wear marks show a depth of 1–3  $\mu\text{m}$  in the roll material. Category 2 consists of rolls that show surface distress and pitting wear. The magnitude of the surface defects show a wide variety of sizes, ranging from small defects in the range of 1  $\mu\text{m}$ , to large holes up to 80  $\mu\text{m}$ . Figure 7 shows pictures of exemplary rolls from the two categories.

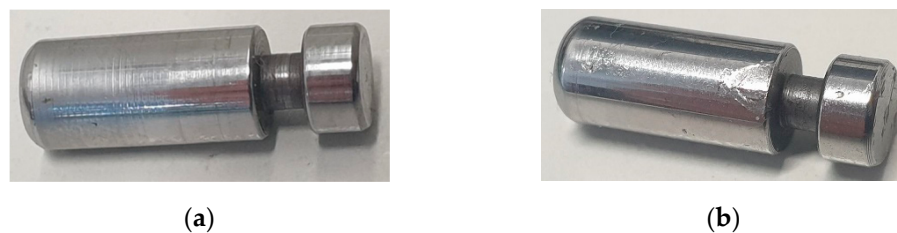


**Figure 7.** Examples of typical wear behaviors in roller burnishing: (a) slightly visible wear marks and (b) surface pitting. Source: own-elaboration.

During the force measurements, both rolls produced a force signal, which was clearly distinguishable from the force signal of a new roll. In particular, the signal-to-noise ratio (SNR) of the force signal could be elaborated as a good indicator on the presence and strength of the roll-wear. As the force signal is oscillating around its optimum value—showing the deviation of the manufactured part from perfect roundness—the SNR in this context can be defined as the ratio of the mean signal amplitude over the standard deviation of the signal.

While the SNR of a new roll was measured to be well above a value of 31, the SNR value decreases with increasing wear marks. While a Category 1 roll with small wear marks around 1  $\mu\text{m}$  already showed a slight decrease in the SNR, the SNR value of a strongly worn roll was found to be decreased by almost 20% compared to the signal of the new roll. Figure 8 shows the raw data signals from all three evaluated rolls, as well as a comprehensive plot showing the signal-to-noise ratios.

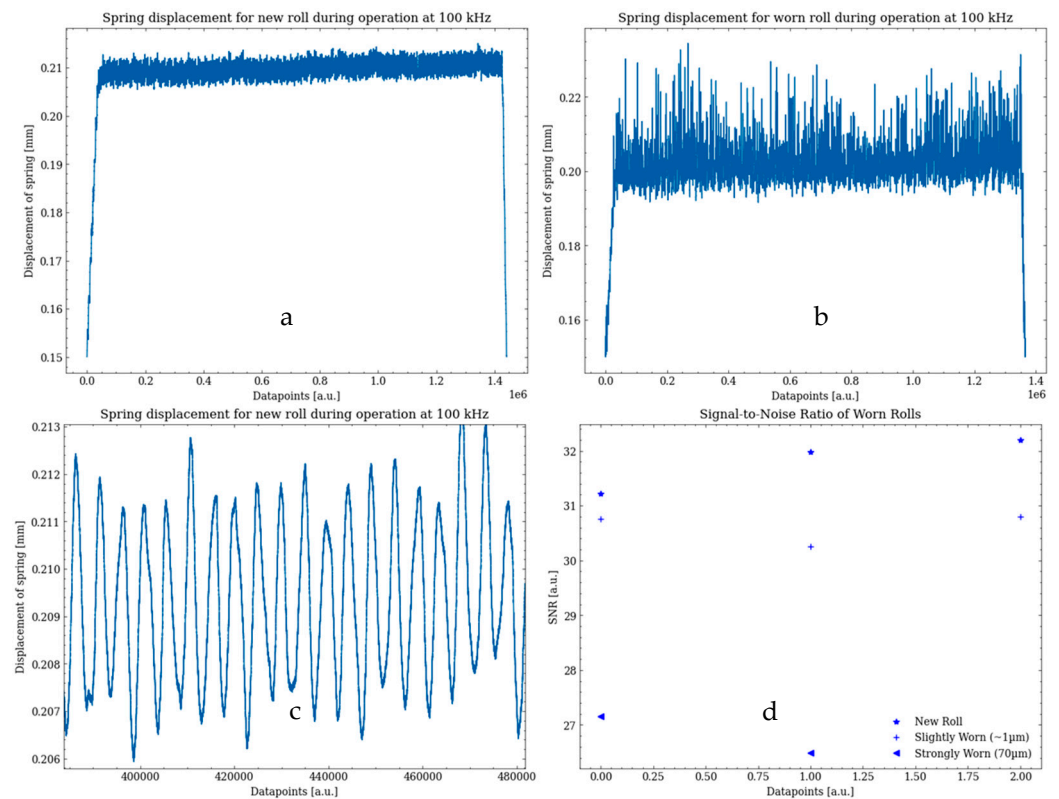


**Figure 8.** Spring displacements of the tool during roller burnishing operations. (a): Displacement signal of a new roll. (b): Displacement signal of a strongly worn roll. (c): Zoom of the displacement signal of a new roll. The signal shows the roundness deviation of the workpiece with an approximate amplitude of 5  $\mu\text{m}$ . (d): Signal-to-noise ratios of the displacement signal from rolls in three different wear states. Stars: New roll. Cross: Roll with slight wear marks of approximately 1  $\mu\text{m}$  in size. Triangle: Worn roll with strong wear marks of approximately 70  $\mu\text{m}$  in size. Source: own-elaboration.

Based on the current results, a method for the monitoring of the tool wear in roller burnishing can be developed by monitoring the signal-to-noise ratio of the tool. Although one of the tested rolls showed only small wear marks, which were only about 1  $\mu\text{m}$  in size, a decrease in the SNR of 3.8% on average was observed in all three trials. A more strongly worn roll yielded an even higher decrease in the SNR of 15.6% and could therefore be clearly distinguished from the new and also from the slightly worn roll. If a corresponding evaluation system is built into the roller burnishing tool, machining processes can be interrupted due to the occurrence of wear, and the production of defect parts can be drastically decreased.

#### 4.3. Communication Benchmark

For a meaningful evaluation of the communication performance, the requirements from the process side to the signal acquisition have to be defined. As was shown in Section 4.1, the signal-to-noise ratio can serve as a sensible metric to distinguish a worn roll from a new roll. Thus, the necessary acquisition frequency for the determination of the SNR needs to be elaborated to derive appropriate communication methods.

The smallest difference in the observed SNRs was between a measurement from a new and a slightly worn roll and was on the order of 0.5. As a rule of thumb, a meaningful measurement system should have a resolution that is 10-times higher than the magnitude of interest. Thus, the goal of the subsequent data processing is to find the minimum acquisition frequency that allows for a correct determination of the SNR. In this study, the SNR at 100 kHz acquisition frequency was considered as the ground truth, and all other

signals were considered relative to this number. Figure 9, the dependence of the calculated SNR from the signal acquisition frequency is shown.

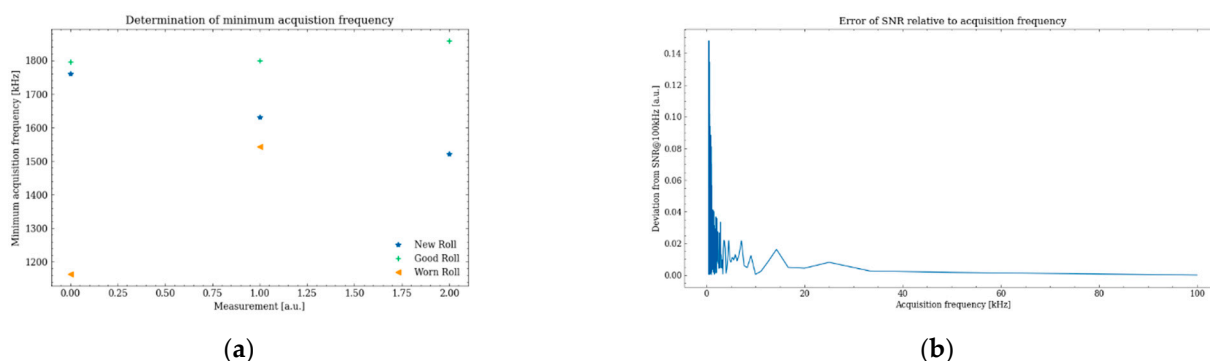


**Figure 9.** Dependence of the calculated signal-to-noise ratio from the acquisition frequency. (a): The minimum acquisition frequency for each dataset. (b): Exemplary plot of the relative deviation of the SNR from SNR@100kHz vs signal acquisition frequency in a range from 500 Hz to 100 kHz. The plots of the other measurements show a similar behavior. Source: own-elaboration.

As shown in Figure 9, the minimum signal acquisition frequency for the correct determination of the SNR is located in a small range of frequencies ranging from 1100 to 1900 Hz for all rolls. We determined this by calculating the frequency at which the determined SNR deviates by more than a predefined value of 0.05 from the SNR at 100 kHz. From 40 kHz onwards, the signal showed only a minimum deviation from the calculated SNR at 100 kHz.

In the following communication benchmark, two scenarios were considered. The potentials of 5G communication technology was investigated with respect to a minimum signal acquisition frequency of 2 kHz, as well as an optimum signal acquisition frequency of 40 kHz. According to the elaborated communication protocol, a status message from the burnishing tool to the machine gateway can have either 18 bytes or 24 bytes. As the 24 bytes message contains slow-varying data, 18 byte messages were considered for the subsequent benchmark.

In a first step, the latency of the 5G network is benchmarked for single 18 byte messages, as well as for a variable package size. The network tests are conducted by the setup described in Section 3.3, with a raspberry pi representing the communication unit attached to the burnishing tool and a virtual machine representing the gateway at the machine tool. On both ends, a small application written in C++ is deployed, which sends generated messages in the defined protocol over 5G via a TCP socket communication.

The latency is measured by the round-trip time from sending a package from the client to the server and back to the client to avoid false measurement results due to imperfectly synchronized clocks on both devices. The measured latency consists of a combination of the application runtime on both ends, as well as the transfer time over the 5G network. Due to a very short runtime of well below 1 ms on both ends, the runtime is not considered any further in the subsequent elaboration.

In order to estimate the required package-size for the determined acquisition frequencies, the general latency of the used 5G-network was tested for different package sizes ranging from 1 byte to 1.6 kilobytes. The observed mean value for the latency was around 10 ms. Considering the elaborated acquisition frequency of minimum 2 kHz and optimally 40 kHz at a size of 4 bytes for each datapoint from the processing force, the required package size was estimated to be between 80 b/package (minimum) and 1600 b/package (optimum). Figure 10 depicts the histograms of the used 5G-network for the described cases.

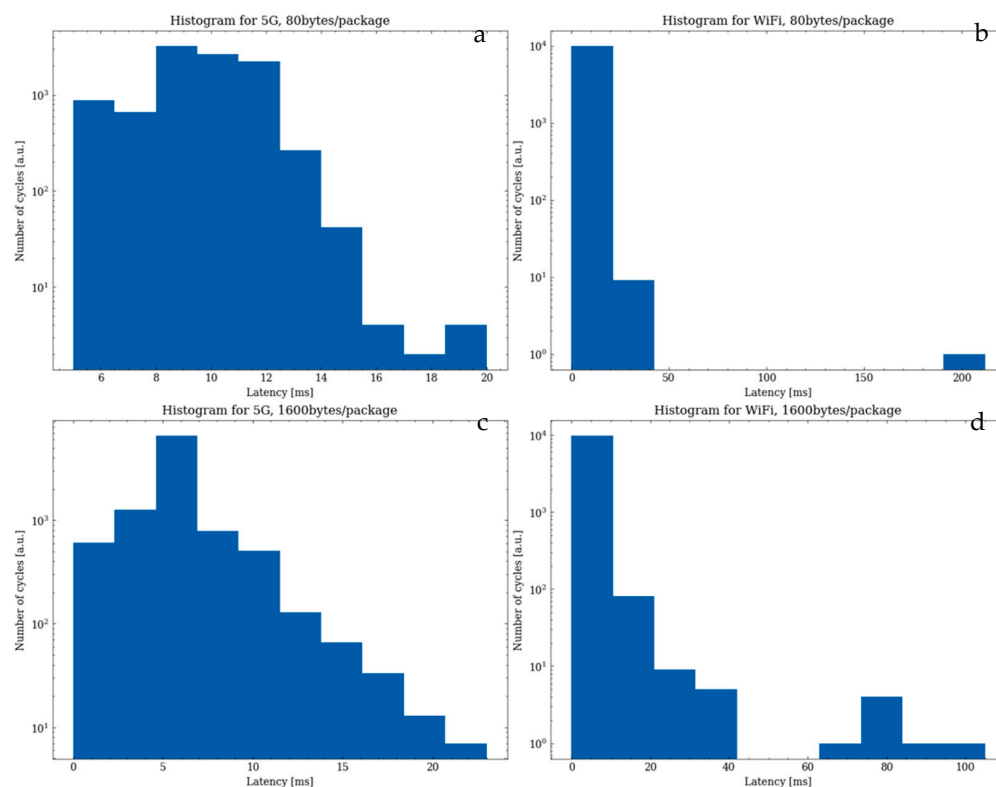


**Figure 10.** Semi-logarithmic histogram plots of 5G communication and conventional 2.4 GHz WiFi communication. Mean values and standard deviation for WiFi: (a):  $1.48 \pm 2.89$  ms (80 bytes), (b):  $4.83 \pm 8.44$  ms (1600 bytes). Mean values and standard deviation for 5G communication: (c):  $9.25 \pm 1.85$  ms (80 bytes), (d):  $5.69 \pm 2.17$  ms (1600 bytes). All histograms were created by a communication by the described protocol with 10,000 data packages for each test. Source: own-elaboration.

From Figure 10, one can see that standard 2.4 GHz WiFi offers a lower medium latency for both use-cases. The strength of 5G lies in the reliability. While the WiFi communication deals with standard deviations, which are twice as high as the medium latency, 5G communication offers very low standard deviations on the order of 2 ms. In standard WiFi communication, single packages need significantly longer (up to 200 ms) than the mean value to be transferred to the server, while in 5G, there was no package observed that needed more than 25 ms.

For an interpretation in the elaborated use-case, reliability is much more important than the actual data rate. If the latency is slightly higher, the package size can be adapted, as long as no compensation for extreme values is required. In order to determine the exact tool-wear in every time-point, 5G communication is the method of choice to ensure a robust and reliable connection.

## 5. Discussion and Outlook

In the present paper, a tool-wear monitoring approach for roller burnishing processes was presented, and a suitable metric based on the signal-to-noise ratio of the processing force was determined. Using the elaborated method, it was possible to distinguish the processing-force signals of rolls with wear marks on the single micrometer scale from new rolls by evaluating the SNR. In particular, the SNR was found to differ by 3.8% on average in the case of very slight wear marks and increased up to a difference of 15.6% on average in the case of a roll with stronger wear marks on the order of 20  $\mu\text{m}$ . For the developed metric, high acquisition frequencies of 2 kHz as a minimum requirement, as well as 40 kHz as an optimum requirement, were found to be necessary to properly differentiate between different wear-states of the burnishing tool.

These high acquisition frequencies offer a challenge to the desired wireless communication method and provided a meaningful industrial use-case for 5G communication. In order to benchmark the benefits of 5G communication technology for the provided use-case, a case study was performed that aimed to measure the latencies for the required conditions. In this study, we found that the most significant benefit of the 5G technology was in the reliability of the communication. While standard 2.4 GHz WiFi communication showed a huge standard deviation of 8.4 ms in the case of 1600 bytes/package and sometimes extremely long communication times, 5G offered a robust communication with highly reliable standard deviations on the order of 2 ms.

In summary, the developed tool concept showed great potential for the monitoring of roller-burnishing processes and provides an interesting use-case for the industrial application of 5G communication technology. In the future, this approach could lead to a higher degree of automation in industrial roller-burnishing processes with fewer defect parts and a lower economic footprint.

In future works, more studies will be performed in order to evaluate the reliability of the elaborated metric under different manufacturing conditions. Further, different alternative communication technologies, such as the novel WiFi 6e standard, should be benchmarked against the 5G standard to elaborate the pros and cons of both technologies in the context of the described use case.

**Author Contributions:** Conceptualization, M.K., D.Z., R.L. and K.M.; experimental results, M.K.; software J.M. (Jacek Mainczyk), J.M. (Jürgen Mansel) and T.S.; data evaluation, M.K. and A.A.; 5G-Tests, A.A., K.I. and M.K.; tool concept, R.L., B.N. and K.H.; electronic concept, J.M. (Jacek Mainczyk), J.M. (Jürgen Mansel) and T.S.; funding acquisition, D.Z. and C.B.; scientific supervision, C.B. and D.Z. All authors have read and agreed to the published version of the manuscript.

**Funding:** This work was performed in the framework of the 5G.NRW project RISEN\_5G, funded by the ministry of economic affairs, innovation, digitalization and energy of the state of North Rhine-Westphalia with the funding-number 2008gif012.

**Acknowledgments:** The authors would like to thank Brunner from Fraunhofer IPT for her support in the CAD design of the developed tool, as well as Mörsen from R&D Steuerungstechnik for his supervision of the project and the great experience he contributed during the development phase.

**Conflicts of Interest:** The authors declare no conflict of interest.

## References

1. El-Axir, M. An investigation into roller burnishing. *Int. J. Mach. Tools Manuf.* **2000**, *40*, 1603–1617. [CrossRef]
2. The Basic Principles of Roller Burnishing. Available online: <https://www.ecoroll.de/en/processes/roller-burnishing.html> (accessed on 16 May 2022).
3. Roller Burnishing and Its Advantages. Available online: <https://www.wenaroll.de/en/technologie/> (accessed on 16 May 2022).
4. Rinaldi, S.; Rotella, G.; Umbrello, D. Experimental and numerical analysis of roller burnishing of Waspaloy. *Procedia Manuf.* **2019**, *34*, 65–72. [CrossRef]
5. The Aim of Roller Burnishing. Available online: <https://www.baublies.com/technology.html> (accessed on 16 May 2022).
6. Sartkulvanich, P.; Altan, T.; Jasso, F.; Rodriguez, C. Finite Element Modeling of Hard Roller Burnishing: An Analysis on the Effects of Process Parameters Upon Surface Finish and Residual Stresses. *J. Manuf. Sci. Eng.* **2007**, *129*, 705–716. [CrossRef]
7. Ecoroll, A.G. Tool Technology for Mechanical Metal Surface Improvement: Cost-effective Processes. Available online: [https://www.ecoroll.de/fileadmin/user\\_upload/Ecoroll\\_AG\\_Product\\_Catalogue\\_E.pdf](https://www.ecoroll.de/fileadmin/user_upload/Ecoroll_AG_Product_Catalogue_E.pdf) (accessed on 16 May 2022).
8. Revankar, G.D.; Shetty, R.; Rao, S.S.; Gaitonde, V.N. Wear resistance enhancement of titanium alloy (Ti-6Al-4V) by ball burnishing process. *J. Mater. Res. Technol.* **2017**, *6*, 13–32. [CrossRef]
9. Kuntoğlu, M.; Aslan, A.; Sağlam, H.; Pimenov, D.Y.; Giasin, K.; Mikolajczyk, T. Optimization and Analysis of Surface Roughness, Flank Wear and 5 Different Sensorial Data via Tool Condition Monitoring System in Turning of AISI 5140. *Sensors* **2020**, *20*, 4377. [CrossRef] [PubMed]
10. Kuntoğlu, M.; Aslan, A.; Pimenov, D.Y.; Usca, Ü.A.; Salur, E.; Gupta, M.K.; Mikolajczyk, T.; Giasin, K.; Kapłonek, W.; Sharma, S. A Review of Indirect Tool Condition Monitoring Systems and Decision-Making Methods in Turning: Critical Analysis and Trends. *Sensors* **2020**, *21*, 108. [CrossRef] [PubMed]
11. Poulachon, G.; Moisan, A.; Jawahir, I.S. Tool-wear mechanisms in hard turning with polycrystalline cubic boron nitride tools. *Wear* **2001**, *250*, 576–586. [CrossRef]

12. Meng, X.; Lin, Y.; Mi, S. The Research of Tool Wear Mechanism for High-Speed Milling ADC12 Aluminum Alloy Considering the Cutting Force Effect. *Materials* **2021**, *14*, 1054. [[CrossRef](#)] [[PubMed](#)]
13. Kermouche, G.; Valiorgue, F.; Rech, J. Correlation of Roller Burnishing Surface Effects with Local Contact Parameters. In Proceedings of the Surface Modification Technologies 2012, Ecully, France, 20–22 June 2012.
14. Narayanan, A.; Ramadan, E.; Carpenter, J.; Liu, Q.; Liu, Y.; Qian, F.; Zhang, Z.-L. A First Look at Commercial 5G Performance on Smartphones. In Proceedings of the Web Conference 2020, Taipei, Taiwan, 20–24 April 2020; pp. 894–905.
15. 5G spectrum Bands Explained—Low, Mid and High Band. Available online: <https://www.nokia.com/networks/insights/spectrum-bands-5g-world/> (accessed on 16 May 2022).
16. The WIRED Guide to 5G. Available online: <http://repositorioir5g.iri.usp.br/jspui/bitstream/123456789/159/1/The%20WIRED%20Guide%20to%205G.pdf> (accessed on 16 May 2022).
17. Trick, U. (Ed.) *5G: An Introduction to the 5th Generation Mobile Networks*; De Gruyter Oldenbourg: Berlin, Germany; München, Germany; Boston, MA, USA, 2021; ISBN 9783110724509.
18. 5G Industry Campus Europe. Available online: <https://5g-industry-campus.com/> (accessed on 16 May 2022).
19. 5G-SMART: Forward Looking Smart Manufacturing Use Cases, Requirements and KPI's. Deliverable D1.1. Available online: <https://5gsmart.eu/wp-content/uploads/5G-SMART-D1.1.pdf> (accessed on 16 May 2022).
20. 5G.NRW Competence Center. Available online: <https://5g.nrw/foerderwettbewerb-5g-nrw-landesregierung-foerdert-13-herausragende-5g-projekte/> (accessed on 16 May 2022).
21. Ansari, J.; Andersson, C.; de Bruin, P.; Farkas, J.; Grosjean, L.; Sachs, J.; Torsner, J.; Varga, B.; Harutyunyan, D.; König, N.; et al. Performance of 5G Trials for Industrial Automation. *Electronics* **2022**, *11*, 412. [[CrossRef](#)]
22. 5G-SMART: Report on Implementation of Options for Monitoring of Workpiece and Machines. Deliverable D3.3. Available online: <https://5gsmart.eu/wp-content/uploads/5G-SMART-D3.3-v1.0.pdf> (accessed on 16 May 2022).